Unsymmetric bistable [c2]daisy chain rotaxanes which combine two types of electroactive stoppers

Adrian Wolf, Juan-José Cid, Emilie Moulin, Frédéric Niess, Guangyan Du, Antoine Goujon, Eric Busseron, Adrian Ruff, Sabine Ludwigs, Nicolas Giuseppone

Unsymmetric bistable [*c*2]daisy chain rotaxanes which combine two types of electroactive stoppers

Adrian Wolf,[a] Juan-José Cid,[a] Emilie Moulin,*[a] Frédéric Niess,[a] Guangyan Du,[a] Antoine Goujon,[a] Eric Busseron,[a] Adrian Ruff,[b, c] Sabine Ludwigs[b] and Nicolas Giuseppone*[a]

[a] SAMS research group, Institut Charles Sadron, CNRS, University of Strasbourg, 23 rue du Loess, BP 84087, 67034 Strasbourg Cedex 2, France, E-mails: emoulin@unistra.fr; giuseppone@unistra.fr, http://sams.ics-cnrs.unistra.fr/
[b] Dr. A. Ruff, Prof. Dr. S. Ludwigs, IPOC-Functional Polymers, Institute of Polymer Chemistry, Universität Stuttgart, Pfaffenwaldring 55, 70569 Stuttgart, Germany
[c] Dr. A. Ruff, present address: Analytical Chemistry – Center for Electrochemical Sciences (CES), Faculty of Chemistry and Bioelectrochemistry, Ruhr University Bochum, Universitätsstr. 150, 44780 Bochum, Germany

Abstract: Mechanically interlocked molecules (MIMs) have emerged as intriguing building blocks for the construction of stimuli-responsive devices and materials. A particularly interesting and well-implemented subclass of MIMs is composed of symmetric bistable [*c*2]daisy chain rotaxanes. Topologically, they consist in the double thread of two symmetric macrocycles that are covalently linked to an axle bearing two switchable stations and a bulky stopper to avoid unthreading. Here we report the synthesis and characterization of a series of unsymmetric bistable [*c*2]daisy chain rotaxanes that present two different electroactive units as stoppers (an electron donor triarylamine and an electron acceptor perylene bisimide unit). Using a combination of 1D and 2D NMR along with cyclic voltammetry, we demonstrate that the pH actuation of the mechanical bond can be used to modulate the electrochemical properties of the bistable [*c*2]daisy chain rotaxanes when switching between the contracted and extended forms.

Introduction

Control of the mechanical bond has been a source of inspiration for molecular and supramolecular chemists over the past thirty years.[1] In particular, the possibility to reach large intramolecular motions by switching interlocked molecules between different stations appears of first interest to access molecular machines.[2,3] For instance, in 2000, Sauvage designed the first topologically double-threaded rotaxane which mimics (at nanoscale) the function of a sarcomere in muscular tissues (at microscale).[4] The so-called [*c*2]daisy chain rotaxane proved to contract or extend by 1.8 nm because of the interplay of transition metal ions binding selectively the two stations with different coordination geometries. This seminal work inspired several other groups (including us) to reproduce the natural contractile motion of muscles up to the macroscopic level.[5–14] Symmetric [*c*2]daisy chain rotaxanes were also used towards functional devices such as logic gates[15] or even plasmonic actuators.[16] However, the design of unsymmetric [*c*2]daisy chain rotaxanes remains unexplored. In this paper, we describe the syntheses and the pH-controlled contraction/extension of unsymmetric [*c*2]daisy chain rotaxanes with two different electroactive stoppers – an electron donor (Figure 1, blue) and an electron acceptor (red). The donor stoppers consist of triarylamine units (TAAs),[17–23] and the acceptor stoppers of unsymmetrical 1,7-dipyrrolidinyl-substituted perylene diimides (PDIs).[24–29] This interlocked structure presents two molecular stations – an ammonium group (orange in Figure 1) and a triazolium group (purple in Figure 1) – with different affinities for the macrocycle.

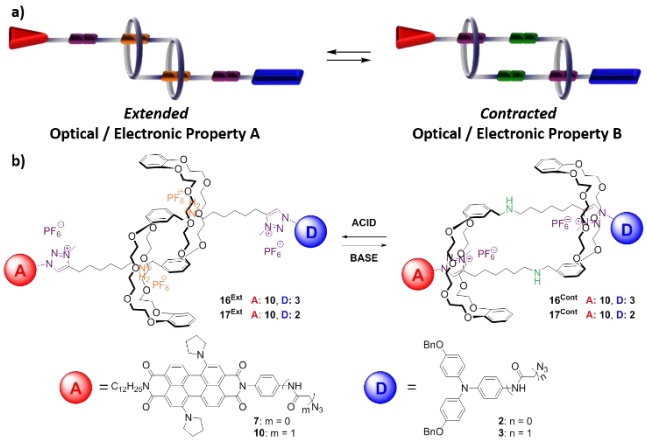

Figure 1. (a) General representation of the mechanical actuation of an unsymmetric [*c*2]daisy chain rotaxane incorporating electron donor (blue) and electron acceptor (red) stoppers; (b) Molecular structures of the pH-switchable [*c*2]daisy chain rotaxanes **16**$^{\text{Ext-Cont}}$ and **17**$^{\text{Ext-Cont}}$.

The mechanical actuation of the [*c*2]daisy chain is based on a strategy developed by Coutrot[30] and already used in our laboratory.[8–10,15] In the protonated state, the macrocycles reside around the ammonium stations *via* ion-dipole and hydrogen

bonding interactions, while, in the deprotonated state, the macrocycles shuttle to the triazolium stations, which are favored over the amine groups. We demonstrate hereafter, using optical spectroscopy and cyclic voltammetry, that a switch between the contracted and the extended forms induces modifications of the optical and electronic properties of the mechanically interlocked rotaxanes.

Results and Discussion

Synthesis of unsymmetric [*c*2]daisy chain rotaxanes

The general synthetic route to access mechanically interlocked molecules **16** and **17** (Figure 1b) involves the introduction of triarylamines **2** or **3** (Scheme 1) and perylene diimides **7** or **10** (Scheme 2) on the pseudo [*c*2]daisy chain rotaxane **11**[31] using a copper catalyzed [3+2] Huisgen cycloaddition reaction (Scheme 3). The corresponding detailed syntheses are described hereafter.

Triarylamine **3** was prepared in three steps and excellent yields from 4-nitro-*N,N*-bis[4-(benzyloxy)phenyl]-phenylamine following previously described protocols of the literature.[15,32] On the other hand, *N,N*-bis(4-(benzyloxy)phenyl) benzene-1,4-diamine **1** was converted into compound **2** in a good yield by a diazotation reaction using sodium nitrite in the presence of hydrochloric acid and followed by aromatic nucleophilic substitution (S_NAr) using sodium azide in deionized water (Scheme 1).

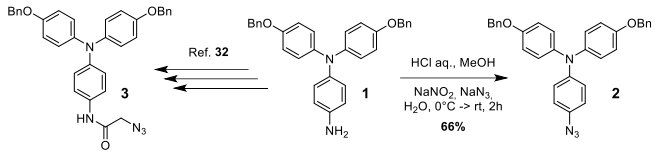

Scheme 1. Synthetic pathways to reach azido-triarylamine derivatives **2** and **3**.

Compounds **7** and **10** were accessed in five and seven steps respectively, in moderate to good yields starting from commercially available perylene-3,4:9,10-tetracarboxylic acid dianhydride (PTCDA) (Scheme 2). Bromination of PTCDA according to literature procedures[33] afforded a crude mixture of the 1,6 : 1,7 : 1,6,7 bromo-isomers in a ratio of 24 : 70 : 6 as indicated by ^{1}H NMR spectroscopy in deuterated sulfuric acid (96–98 % w/w solution in D_2O). The crude mixture was then diimidated using *n*-dodecylamine in *N*-methylpyrrolidinone (NMP) in the presence of acetic acid at 120 °C for 19 hours. An isomeric mixture of 1,6 and 1,7 isomers of diimide **4** (1,6:1,7-**4**) in a ratio of about 1 : 4 (estimated by ^{1}H NMR spectroscopy) was obtained in 48 % yield over two steps. The isomers could not be separated at this stage by flash column chromatography and thus, the mixture was used as such in the next step. Subsequent S_NAr of the bromide groups by pyrrolidine provided dipyrrolidinated diimide 1,6-**5** and 1,7-**5** in 13 % and 38 % yields, respectively (the two isomers were separated by column chromatography at that stage). Compound 1,7-**5** was then mono-saponified using potassium hydroxide in *tert*-butanol under reflux for 10 minutes to give the key intermediate **6** in 63 % isolated yield.[29] Compound **7** was then obtained in one step and 85 % yield from **6** *via* imidation with 4-aminophenylazide.[34] Alternatively, imidation of **6** with *p*-phenylenediamine gave unsymmetrical PDI **8** in quantitative yield, which was further chloroacetylated to form compound **9** in 89 % yield using equimolar amounts of 2-chloroacetyl chloride and triethylamine in dichloromethane. Finally, after stirring compound **9** with sodium azide in *N,N'*-dimethylformamide at 80 °C for 25 hours, we obtained azido-functionalized perylene diimide **10** in 70 % yield.

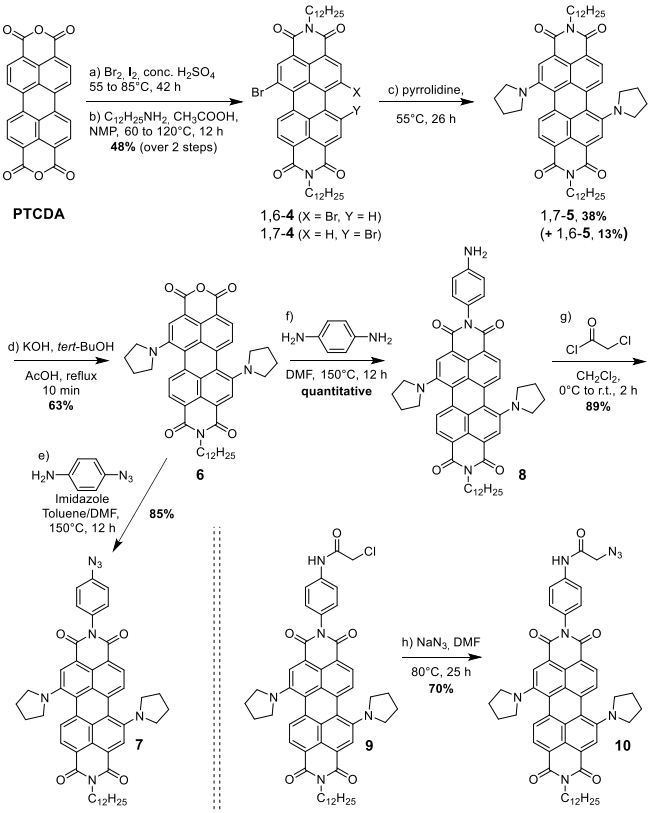

Scheme 2. Synthetic route towards unsymmetric perylene bisimide **7** and **10**.

The reaction pathways to access (non-methylated) triazole rotaxanes **12-15** are shown in Scheme 3. In the one pot version (Scheme 3a), the bisalkynyl-substituted pseudorotaxane **11**[30,31] was reacted with azido-substituted triarylamine **2** or **3** and azido-substituted perylene **7** or **10** via [3+2] Huisgen cycloaddition using a 1:1:1 (**11** / (**2** or **3**) / (**7** or **10**)) stoichiometric ratio. Unfortunately, all reaction conditions used to couple compound **7** failed probably due to the strong delocalization of electrons in the perylene ring making the azido group unreactive. The reactions involving **10** were carried out in the presence of 2,6-lutidine and tetrakisacetonitrile copper(I) hexafluorophosphate in dichloromethane at room temperature for 3–4 days. They satisfyingly gave the desired triarylamine-perylene diimide (TAA-PDI) systems **14** and **15** in 25 % and 10 % isolated yields, respectively. The difficulty of this one-pot approach to prepare unsymmetrical systems **14** and **15** relied on the purification of the crude reaction mixtures, which contained at least five different species on TLC. Several factors account for this very complex mixture: 1) the presence of stereoisomers of the [c2]daisy chain unit;[31] 2) the formation of mono-coupled cycloadducts between **10** and **11** as well as between **2** or **3** and **11**; 3) the formation of bis-coupled cycloadducts between **10** and **11** as well as between **2** or **3** and **11**; and 4) the presence of residual amounts of unreacted starting materials. Purification of **14** and **15** was however accomplished by conventional flash column chromatography on silica gel. First, elution with pure dichloromethane was used to remove unreacted triarylamine **2** or **3** and PDI **10**. Then, a ternary eluent mixture of dichloromethane, methanol and toluene starting with a ratio of 100 : 0 : 2 and increasing polarity slowly up to 100 : 5 : 2 allowed the sequential removal of 1) [**2+11+2**] or [**3+11+3**];[15] 2) mono-coupled cycloadducts ([**2+11**] or [**3+11**]), and 3) desired compound **14** or **15**. Further elution with increasing polarity afforded PDI derivatives [**10+11**] and [**10+11+10**].

Alternatively, we envisioned a sequential approach involving first the formation of mono-coupled cycloadducts [**2+11**], [**3+11**] or [**10+11**] as intermediates (Scheme 3b for [**10+11**]). In this stepwise approach, 4.7 equivalents of **11** were first stirred with either one equivalent of **2**, **3** or **10** for three days in the presence of one equivalent of tetrakisacetonitrile copper(I) hexafluorophosphate and 2,6-lutidine in dichloromethane to give the intermediates [**2+11**], [**3+11**] or [**10+11**] in 32 %, 19 % and 32 % isolated yields, respectively. For the synthesis of [**2+11**] and [**3+11**], the side-products resulted only in excess quantities of **11** and a small amount of [**2+11+2**] or [**3+11+3**] (see SI). For the synthesis of [**10+11**], bis-coupled cycloadducts [**10+11+10**] could not be detected by LC-MS. The second step was then tested between [**10+11**] and **2** which were mixed in a 1 : 1 stoichiometric ratio in dichloromethane for three days in the presence of an equimolar amount tetrakisacetonitrile copper(I) hexafluorophosphate and 2,6-lutidine. In this way, compound **15** was obtained in 30% yield after an easier chromatography column.

Finally, the triazole groups in **14** and **15** were selectively methylated in the 3 position using a mixture of methyl iodide and dichloromethane over 4 days, followed by anion exchange using ammonium hexafluorophosphate to give the extended systems **16^{Ext}** and **17^{Ext}** in 80 % and 94 % yields, respectively (Scheme 4, top). Deprotonation of these compounds to the contracted

form, **16^{Cont}** and **17^{Cont}**, was accomplished using a biphasic mixture of 0.1 M aqueous sodium hydroxide and dichloromethane at room temperature for 1 hour and proceeded in 95 % yield (Scheme 4, bottom). Compounds **16^{Cont}** and **17^{Cont}** proved less soluble in acetonitrile than their extended forms **16^{Ext}** and **17^{Ext}**.

Characterization of [c2] daisy chain rotaxanes 16 and 17

All compounds were characterized by ^{1}H and ^{13}C NMR and by either ESI or MALDI-TOF mass spectroscopy (see Experimental Section and SI for ^{1}H and ^{13}C NMRs of key compounds). In order to probe the contraction/extension event of the unsymmetric [*c*2] daisy chain rotaxanes, a precise determination of the ^{1}H signals of compounds **16** and **17** is necessary. This was achieved thanks to a combination of standard 1D and 2D NMR techniques on most of the synthetic intermediates and particularly on compounds **2**, **3**, **10**, **14** and **15**. For compounds **2** and **3**, the ^{1}H NMR spectra of the aromatic region was assigned based mainly on the integration of the aromatic proton signals of the triarylamine unit and on ^{1}H-^{1}H COSY NMR (Figure 2 and SI).

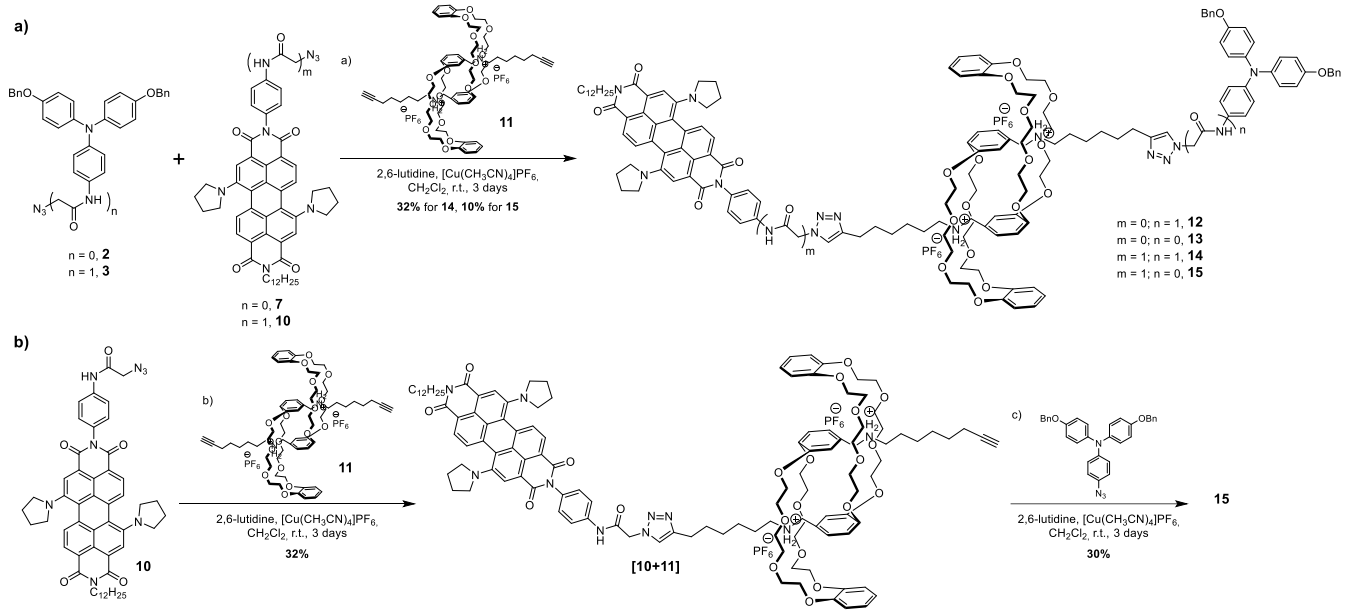

Scheme 3. a) One-pot synthetic route towards unsymmetrical [*c*2] daisy chain rotaxanes **12-15**; **b)** Sequential synthetic route towards unsymmetrical [*c*2] daisy chain rotaxane **15**.

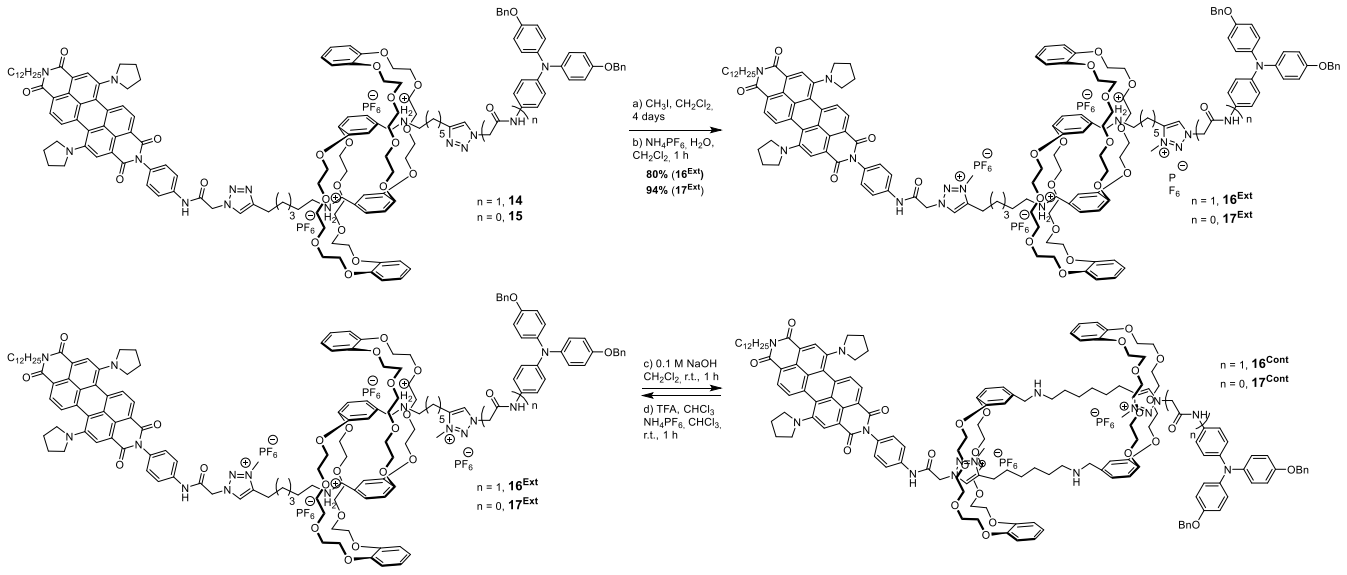

Scheme 4. Synthetic route towards unsymmetric [*c*2] daisy chain rotaxanes **16** and **17** and their subsequent acid/base controlled actuation.

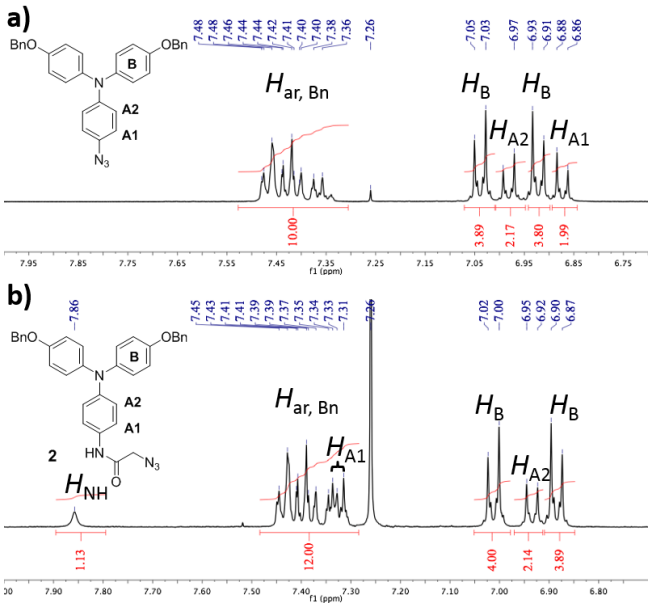

Figure 2. Partial ^{1}H NMR spectra (400 MHz, $CDCl_3$, 25 °C) of compounds **2 (a)** and **3 (b)** with chemical shift assignments.

For both compounds, the aromatic protons of the Bn group showed a multiplet between 7.50 and 7.30 ppm while the two doublet peaks integrating for 4 each at δ ~ 7.04 and 6.92 ppm were assigned to the phenyl ring B.[35] For compound **3**, one doublet with an integral of 2 was found strongly shifted towards the low-field region of the spectrum compared to **2** and was thus assigned to proton H_{A1}. The other doublet at δ ~ 6.97 ppm in between the two H_B protons was assigned to H_{A2}. For compound **10**, the use of ^{1}H and/or ^{1}H-^{1}H COSY NMRs on all synthetic intermediates from compound 1,7-**5** was necessary to precisely determine the different proton signals (Figure 3 and SI for ^{1}H and COSY NMRs of compounds **5**, **6**, **8**, **9** and **10**). Below, we describe only the ^{1}H NMR spectrum of compound **10**. Two singlets are observed for H_{A1} and H_{D1}. Compared to proton A1, the chemical shift of proton D1 should not be affected during the whole synthetic sequence from 1,7-**5** to **10** and thus, based on ^{1}H NMR spectra, the lowest field singlet (δ = 8.48 ppm) was ascribed to H_{A1} while the highest field one (δ ~ 8.39 ppm) was ascribed to H_{D1}. Protons $H_{B1,B2}$ and $H_{C1,C2}$ were identified based on their multiplicity (doublet) and on COSY correlations. Aromatic *ortho* or *bay* protons were discriminated based on their proximity to the electron-withdrawing imide groups. Namely, the low-field shifted doublets (δ ~ 8.41-8.36 ppm) was assigned to the *ortho* protons (H_{B1} and H_{C1}) as they experience a stronger deshielding effect from the imide group compared to the *bay* protons (H_{B2} and H_{C2}), which thus appear at higher field (δ ~ 7.63, 7.57 ppm). Protons H_{B2} and H_{C2} (and respectively H_{B1} and H_{C1}) were then identified following a similar reasoning to the one made for H_{A1} and H_{D1}, i.e. H_B protons are shifted to higher field compared to H_C protons. Protons H_{E1} and H_{E2} were identified based mainly on their integrations compared to all protons from the perylene core. The more downfield shifted signal was attributed to protons H_{E2}, because the H_{E1} ones, closer in space to the free primary amine group, might experience a greater shielding effect resulting in a lower resonance frequency. Finally, the amide proton (H_{am}) was clearly evidenced when comparing ^{1}H NMR spectra of compounds **9** and **10**. In the aromatic region, this proton signal exhibits an upfield shift ($\Delta\delta$ = - 0.16) from 8.44 ppm in PDI **9** to 8.28 ppm in PDI **10**. This observation probably results from an increased electron density on the nitrogen from the azide involved in hydrogen bonding compared to the chlorine atom, thus causing the shielding effect that makes the amide proton in **10** resonate upfield shifted compared to PDI **9**. This observation is in good agreement with the upfield shift ($\Delta\delta$ = -0.07 ppm; from δ = 4.23 to 4.16 ppm) observed for the protons in the α position (H_α).

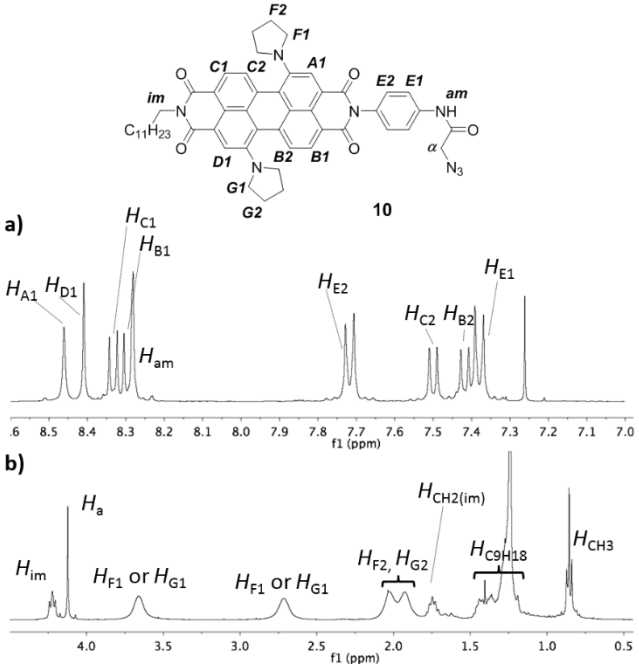

Figure 3. Partial ^{1}H NMR spectra (400 MHz, $CDCl_3$, 25 °C) of compound **10** with chemical shift assignments a) in the low-field region from 8.6 to 7.0 ppm and b) in the high-field region from 4.5 to 0.5 ppm.

Our experience with molecules based on [*c*2]daisy chain rotaxane **11**,[8,9,15] together with the precise determination of the ^{1}H signals of compounds **2** and **10** and complemented by ^{1}H-^{1}H COSY NMR allowed us to assign all protons on compound **14** from their chemical shifts in $CDCl_3$ (Figures S16 and S17). However, the solubility of the unsymmetric [*c*2]daisy chain rotaxane **15** proved to be quite limited in *d*-chloroform and thus ^{1}H and ^{1}H-^{1}H COSY NMR in CD_3CN were used to precisely assign the different proton signals of compound **15** (Figures S19 and S20). Methylation of compounds **14** and **15** did not greatly affect their ^{1}H NMR spectra, which displayed mainly a downfield shift of the signals corresponding to the protons of the triazole units (from δ ~ 7.50 ppm to δ ~ 8.20 ppm) and the appearance of new singlets at δ ~ 4.20-4.10 ppm corresponding to the methyl groups on the triazole (Figures 4a, S20a, and S21a).

We then probed the pH-controlled contraction/extension for **16** and **17** by ^{1}H NMR. Figure 4 shows a comparison between the ^{1}H NMR spectra of **16^{Ext}** and **16^{Cont}** in CD_3CN. The signals assigned to the vinylic protons of the triazolium groups (T1 and T1') and to the methylene protons in between the amide and triazolium units (α and α') show downfield shifts going from the extended state (**16^{Ext}**) to the contracted state (**16^{Cont}**) as a result of the shuttling motion of the macrocycles from the ammonium stations to the triazolium stations. Furthermore, the benzylic methylene protons (9 and 9') next to the ammonium station and the methylene protons (3 and 3') next to the triazolium station show up- and downfield shifts, respectively (green dashed lines). These observations are in agreement with what was observed for other molecules based on [*c2*] daisy chain rotaxane **11**.[8,9,15,31] Similar observations were made for compounds **17^{Ext}** and **17^{Cont}**, regarding the vinylic protons of the triazolium groups, the methylene protons in between the amide and triazolium units, the benzylic methylene protons next to the ammonium station and the methylene protons next to the triazolium station (Figure S22).

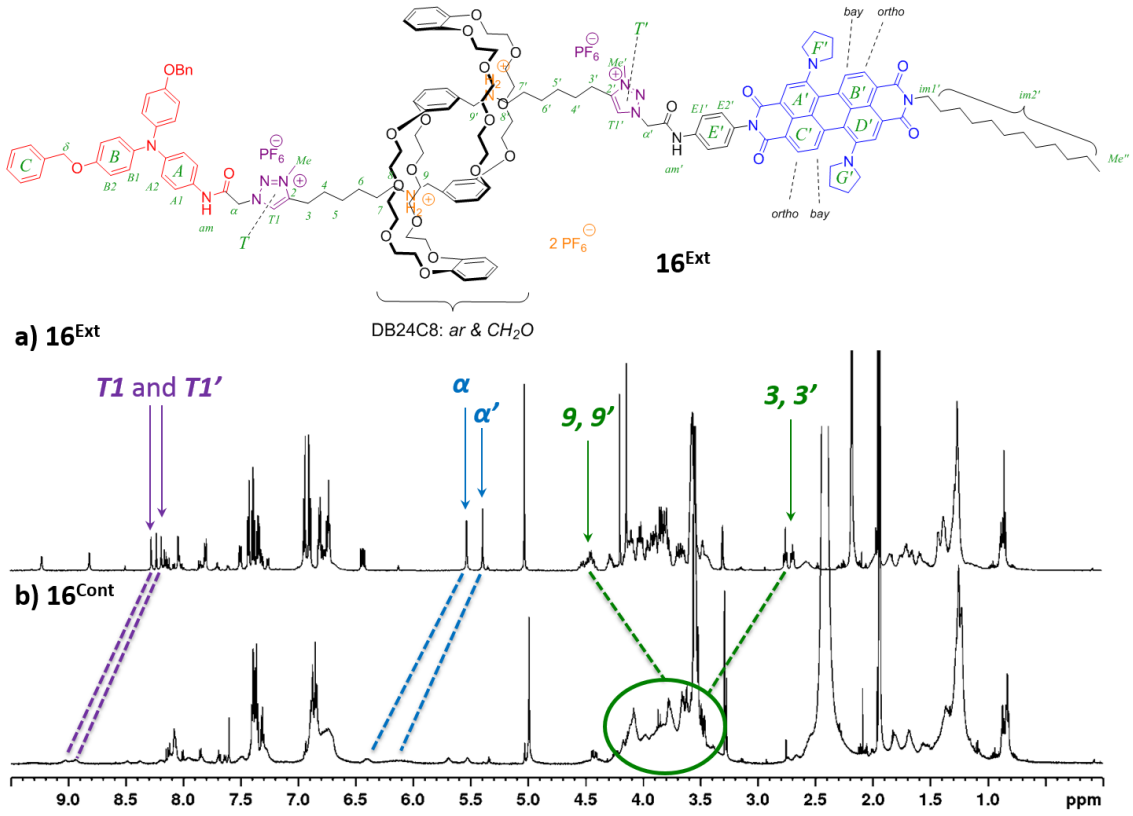

Figure 4. ^{1}H NMR spectra (400 MHz, CD_3CN, 25 °C) of compounds a) **16^{Ext}** and b) **16^{Cont}** showing different chemical shifts between extended and contracted states. The purple, blue and green dashed lines indicate important shifts of protons influenced by the shuttling of the macrocycles.

We also used ^{1}H DOSY NMR spectroscopy to confirm the contraction/extension event on compound **16** (Figure 5). DOSY NMR experiments provide information on the diffusion behavior of the molecules and thus on their hydrodynamic radii (R_H) using the Stokes-Einstein equation which considers a hard sphere model. For the extended state, a lower diffusion coefficient is expected compared to the contracted state. DOSY NMR spectra confirmed the presence of a single diffusing species in both the contracted and extended forms. Diffusion coefficients (D) of 247 $\mu m^2 s^{-1}$ and 343 $\mu m^2 s^{-1}$, which correspond to hydrodynamic radii R_H of 2.47 and 1.78 nm, were measured for **16^{Ext}** and **16^{Cont}**, respectively. This result is consistent with the expected extended and contracted states and confirms the occurrence of the contraction/extension event upon pH modulation. This stands also for compound **17** (see Figure S3).

We then studied the optical properties of the unsymmetric rotaxanes by means of UV-Vis-NIR absorption and fluorescence experiments. UV-Vis-NIR absorption spectra of compounds **16^{Ext}** and **16^{Cont}**, together with references **3** and **9**, were recorded in chloroform, a solvent in which all components display a good solubility (Figure 6 and S1a). We found that reference compound **3** absorbs light below 400 nm while perylene **9** displays a maximum of absorption at 705 nm with a small shoulder at 645 nm, corresponding to the S_0-S_1 electronic transition, along with a higher energy S_0-S_2 electronic transition at 436 nm, in agreement with the literature.[24] Overall, we found that the absorption spectra of **16^{Cont}** correspond well to the sum of its reference components in the contracted state. However, for compound **16^{Ext}**, a bathochromic shift of the absorbance corresponding to the S_0-S_1 electronic transition (725 nm) was observed (Figure 6a). Compared to reference perylene **9** and compound **16^{Cont}**, such behavior can suggest the formation of J-aggregates in the extended state. However, for compounds **17^{Ext}** and **17^{Cont}** in benzonitrile, the actuation did not lead to significant differences by UV-Vis spectroscopy (Figure S1b).

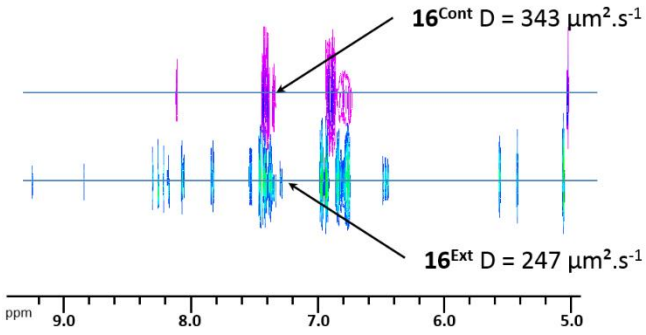

Figure 5. Partial DOSY NMR spectra of compounds **16^{Ext}** and **16^{Cont}** (400 MHz, CD_3CN, 25 °C) showing differences in the diffusion coefficient between extended and contracted states.

Steady-state fluorescence experiments on compounds **9**, **16^{Ext}** and **16^{Cont}** were also recorded in chloroform after excitation at 440 nm (Figure 6 and S1c). The fluorescence spectrum of extended compound **16^{Ext}** shows a maximum of emission at 773 nm, which is red-shifted by 39 nm compared to the fluorescence spectrum of reference perylene compound **9**. Interestingly, for contracted compound **16^{Cont}**, the maximum of emission was located at around 753 nm, which is blue-shifted by 20 nm compared to its extended counterpart **16^{Ext}**. Furthermore, we can note that the intensity of emission is enhanced for the contracted rotaxane compared to the extended one. These observations are in agreement with the steady-state absorption studies and suggest that, in the extended state, aggregation of the perylene units occurs while in the contracted one, the presence of the crown ether macrocycle in the vicinity of the perylene unit prohibits this phenomenon.

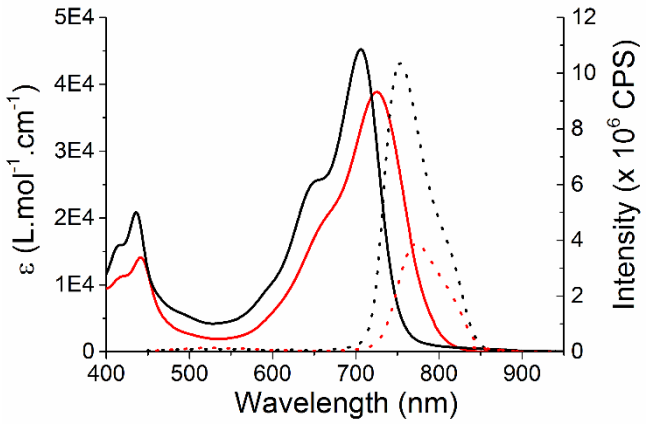

Figure 6. Molar absorbance coefficient (plain line) and fluorescence spectra (dashed line) upon excitation at 440 nm of rotaxanes **16^{Ext}** (red) and **16^{Cont}** (black) recorded in chloroform at a concentration of 0.1 mM.

Finally, the electrochemical behavior of compounds **16** and **17** including the determination of reduction and oxidation potentials to define their energy levels and electronic properties was probed by cyclic voltammetry in 0.1 M NBu_4PF_6/CH_2Cl_2 at a gold disk electrode under planar diffusion conditions (Figures 7 and S2). Cyclic voltammograms of **16^{Ext}** (Figure 7a, black trace) show a chemical reversible reduction process with a mid-point potential $E_{1/2,c}$ centered at -1.30 V vs. Fc/Fc^+ (Table 1) and two chemically reversible oxidation processes with mid-point potentials ($E_{1/2,a}$) of +0.19 V and +0.31 V vs. Fc/Fc^+. The higher peak amplitude of the first oxidation process indicates an overlap of the oxidation of the TAA unit and the first oxidation of the perylene unit. This becomes obvious by comparing the redox potential of the isolated perylene (**S2**) and triarylamine (**S4**) reference compounds (Figure S2) that reveal mid-point potentials for the oxidation of +0.17 and +0.30 V (both **S2**) and +0.17 V (**S4**). Due to the blocking of the *para*-positions in the triarylamine stopper no follow-up reactions such as dimerization occur.[36,37] Moreover, the pronounced current amplitude of the reduction of the perylene unit in the reference compound **S2** that is about twice the current amplitude of the first oxidation process in **S2** (Figure S2a) strongly suggests a two-electron transfer mechanism for the cathodic process. Evidently, the cyclic voltammetric response of the extended form **16^{Ext}** reflects the voltammetric signatures of the individual reference compounds **S2** and **S4** and significant effects of the macrocycle on the electrochemical response of the electroactive stoppers are absent. Consequently, the donor and acceptor site can be regarded as isolated redox sites within the daisy chain rotaxane in **16^{ext}**. On the other hand, the contracted form **16^{Cont}** (Figure 7a, red trace) shows a rather broad reduction wave of low chemical reversibility and only a rather broad chemically reversible oxidation wave. The crown ether-based

macrocycle seems to significantly alter the electrochemical response of the redox active stoppers in the contracted conformation. In case of the reduction the closer proximity of the crown ether moiety seems to have a destabilizing effect on the reduced perylene stopper form. This is seen from the weak re-oxidation peak in the backward scan of the reduction suggesting lower chemical stability. Comparing the oxidation waves of the extended and contracted forms one sees that the potential of the second oxidation of the perylene unit is shifted to lower potentials which results in a stronger superposition with the first oxidation of the perylene and the TAA stopper. A lower potential for this second oxidation does also indicate easier oxidation in the contracted form compared to the extended one.

The electrochemical response of **17**^{Ext} (Figure 7b, black trace) and **17**^{Cont} (red trace) shows a similar behavior. However, the effect of the crown ether moiety seems to be less pronounced. Cyclic voltammograms of **17**^{Ext} show a single chemically reversible reduction process located at -1.33 V vs. Fc/Fc^+ (Table 1) in analogy to **16**^{Ext}. However, in the contracted form, a peak splitting was observed that might be attributed to an interaction of the macrocycle with the singly reduced perylene unit. In contrast to **16**^{Ext}, here, the macrocycle seems to have a stabilizing effect on the radical anion and shifts the potential of the second reduction to more negative values (-1.45 V vs. Fc/Fc^+). A similar effect on the potential was observed for the oxidation processes. The mid-point potentials of the oxidation processes (stepwise oxidation of the perylene unit and $1e^-$ oxidation of the triarylamine unit) are shifted to more positive values when going from **17**^{Ext} (+0.13 V, +0.27 V and +0.36 V) to **17**^{Cont} (0.18 V, 0.31 V and 0.41 V). Comparison with the model compound **S3** (isolated triarylamine unit, $E_{1/2,a}$ = +0.3 V, Figure S2) suggests that the second oxidation process is most likely located at the triarylamine based stopper.

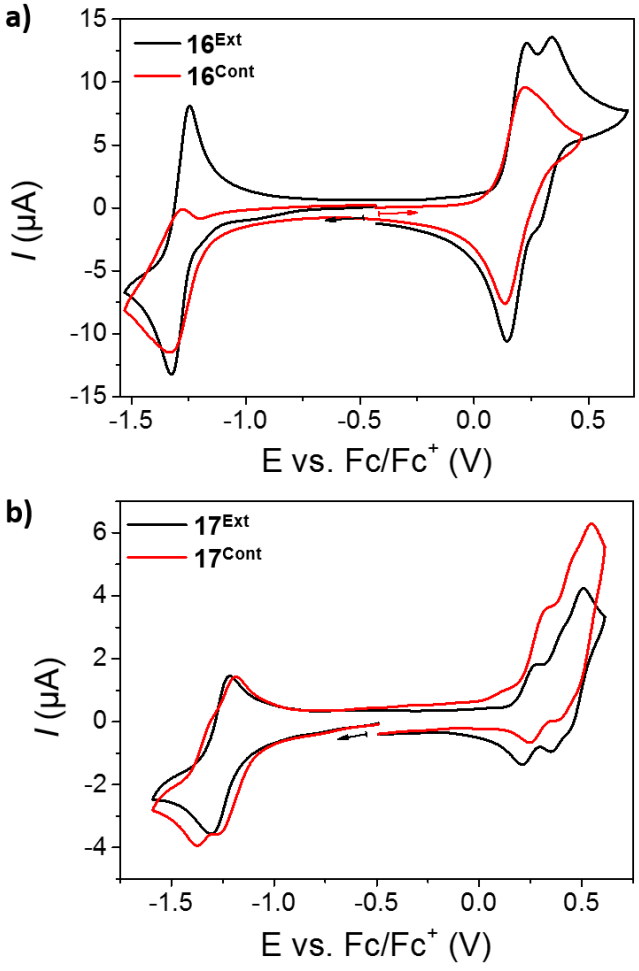

Figure 7. Cyclic voltammograms of compounds **16** (a) and **17** (b) in 0.1 M NBu_4PF_6/CH_2Cl_2 at a gold disk electrode (planar diffusion conditions). a) **16**^{Ext} (c = 0.74 mM), **16**^{Cont} (c = 0.77 mM); b) **17**^{Ext} (c = 0.25 mM), **17**^{Cont} (c = 0.28 mM); all voltammograms were recorded with a scan rate of 100 $mV.s^{-1}$ and were not background corrected; arrows indicate initial scan direction.

Although not fully deciphered, the difference in the electrochemical behavior between the extended and contracted forms can be attributed to the shuttling of the crown ether in the vicinity of the redox unit and thus: *i*) change the solvation shell around it; *ii*) induce van der Waals or H-bonds interactions; and *iii*) have a general shielding effect on the structural rearrangement upon electron transfer. All these effects will lead to a change in the reorganization energy upon reduction / oxidation and can also

change the kinetics of the electron transfer interactions which can induce peak splitting, as for instance observed for the reduction of **17^{Cont}**. The differences in the electrochemical response between the extended and contacted forms should in principle allow for an electrochemical identification of the individual species under acidic or basic conditions and shows the potential applicability of this system in e.g. pH sensitive sensor devices based on an electrochemical readout. It should be here mentioned that such an altered electrochemical response of redox active rotaxane upon protonation/deprotonation was recently reported for a [2]rotaxane equipped with redox active viologen units.[38]

From the estimated mid-point potentials, the HOMO (highest occupied molecular orbital) and LUMO (lowest unoccupied molecular orbital) energy levels (E_{HOMO} and E_{LUMO}) were calculated for the electron donor-acceptor systems **16** and **17** (Table 1, for details on the calculation see Supporting Information). The lowest HOMO value was observed for **16^{Ext}** (5.28 eV). The highest LUMO level was found for **17** (both forms, 3.77 eV). The electrochemical band gaps, determined from the differences in energy levels, ranged from 1.46 to 1.51 eV. These values are even above the values for TAA-fullerenes dyads and triads ($E_{CV, gap}$ = 1.31 – 1.34 eV) and demonstrate the strong electron affinity of the perylene unit.[32]

Table 1. Mid-point potentials of the oxidation ($E_{1/2,a}$) and reduction processes ($E_{1/2,c}$), energy levels (E_{HOMO} and E_{LUMO}) and electrochemical band gap ($E_{CV, gap}$) values for compounds **16** and **17** determined in 0.1 M NBu_4PF_6/CH_2Cl_2 at a planar Au disk electrode with a nominal diameter of 3 mm. All potentials were given vs. the potential of the Fc/Fc^+ redox couple.

	$E_{1/2,a}$ (V)[a]	$E_{1/2,c}$ (V)	E_{HOMO} (eV)[b]	E_{LUMO} (eV)[b]	E_{gap} (eV)[c]
16^{Ext}	+0.19 (+0.31)	-1.30	-5.29	-3.81	1.48
17^{Ext}	+0.13 (+0.27) (+0.36)	-1.33	-5.23	-3.77	1.46
16^{Cont}	+0.18	-1.31	-5.28	-3.80	1.48
17^{Cont}	+0.18 (+0.31) (+0.41)	-1.33 (-1.45)	-5.28	-3.77	1.51

[a] Values in parentheses correspond to the mid-point potentials of the second and third oxidation. [b] E_{HOMO} (=-($E_{1/2,a}$+5.1)[eV]) and E_{LUMO} (=-($E_{1/2,c}$+5.1)[eV]) values were calculated from the mid-point potentials of the first oxidation or reduction process, respectively; the error in potential values is estimated to be ≤ ± 0.01 V. [c] E_{gap} calculated as the difference between the HOMO and LUMO level.

Conclusions

To summarize, we have designed and synthesized two unsymmetrical pH-switchable [*c*2]daisy chain rotaxanes which combine electroactive triarylamine and perylene units as stoppers. Using 1D and 2D NMR spectroscopies, we have demonstrated the efficiency of the shuttling process upon stepwise addition of base and acid. This advanced synthetic example shows that complex [*c*2]daisy chains bearing distinct substituents can enrich the number of chemical structures within that family of compounds. In addition, cyclic voltammetry experiments show that the electrochemical properties of such [*c*2] daisy chain rotaxanes can be altered by the shuttling event occurring upon pH modulation. It can be anticipated that the electrochemical discrimination - although not pronounced but clearly visible - of the two conformations allow for the use of such supramolecular structures in pH sensitive electrochemical sensor devices. Moreover, the unsymmetrical nature of the redox active daisy chain rotaxanes based on the integration of an electron donor (triarylamine) and an electron acceptor (perylene) unit allows for the selective electrochemical triggering of only a single stopper unit and may thus be of particular importance for the fabrication of complex electrochemically active molecular machines.

Experimental Section

General methods. All reactions were performed under an atmosphere of argon unless otherwise indicated. All reagents and solvents were purchased at the highest commercial quality and used without further purification unless otherwise noted. Dry solvents were obtained using a double column SolvTech purification system. Yields refer to purified spectroscopically (^{1}H NMR) homogeneous materials. Thin Layer Chromatographies were performed with TLC silica on aluminium foils (Silica Gel/UV254, Aldrich). In most cases,

irradiation using a Bioblock VL-4C UV-Lamp (6 W, 254 nm and/or 365 nm) as well as *p*-anisaldehyde, phosphomolybdic acid and Cerium ammonium molybdate stainings were used for visualization. Ultra Performance Liquid Chromatographies coupled to Mass Spectroscopy (UPLC-MS) were carried out on a Waters Acquity UPLC-SQD apparatus equipped with a PDA detector (190-500 nm, 80Hz), using a reverse phase column (Waters, BEH C18 1.7 µm, 2.1mm x 50 mm), and the MassLynx 4.1 – XP software. MALDI mass spectra were recorded on a Bruker Daltonics Autoflex II TOF spectrometer. High resolution mass spectra were recorded on a Micro-Q-TOF apparatus from Bruker. ^{1}H NMR spectra were recorded on a Bruker Avance 400 spectrometer at 400 MHz and ^{13}C spectra at 100 MHz in $CDCl_3$ or CD_3CN at 25°C. The spectra were internally referenced to the residual proton solvent signal ($CDCl_3$: 7.26 ppm and CD_3CN: 1.94 ppm for ^{1}H spectrum, and $CDCl_3$: 77.16 ppm and CD_3CN: 118.26 and 1.32 ppm for ^{13}C spectrum). For ^{1}H NMR assignments, the chemical shifts are given in ppm. Coupling constants *J* are listed in Hz. The following notation is used for the ^{1}H NMR spectral splitting patterns: singlet (s), doublet (d), triplet (t), multiplet (m), large (l). *Diffusion Order Spectroscopy (DOSY) NMR spectra* were recorded on a Bruker Avance I spectrometer at 500 MHz at the Service de Résonance Magnétique Nucléaire at the Faculty of Chemistry at the University of Strasbourg. *UV-Vis-NIR spectra* were recorded on either Cary 500 Scan Varian or Perkin Elmer – Lambda 25 UV-Vis-NIR spectrophotometers in a quartz glass cuvette with 1.0 cm optical path. *Fluorescence emission spectra* were recorded on a FluoroMax-4 (Horiba JobinYvon) spectrofluorometer with the following settings: slit width = 5 nm, increment = 1 nm, integration time = 0.1 s in a quartz glass cuvette with a 1.0 cm optical path. *Cyclic Voltammetry experiments* were recorded according to the protocol reported in the Supporting Information.

Compound 2: To a stirred, sticky suspension of **1** (188 mg, 398 µmol) in MeOH (5 mL) was added slowly a 1 M HCl solution (6 mL) followed by two drops of conc. HCl. The mixture was then cooled down to 0°C. After 15 min at this temperature, $NaNO_2$ (129 mg, 1.87 mmol) in water (0.8 mL) was added dropwise within about 2 min. The yellow-orange suspension immediately turned brown after the first drop. The mixture was further stirred for 35 min. Then, NaN_3 (259 mg, 3.98 mmol) in water (2.6 mL) was added in two portions. The brown suspension was further stirred for 40 min, while allowing the mixture to warm up to room temperature. Dichloromethane (90 mL) was added and the mixture was washed with water (90 mL). The organic phase was washed with sat. $NaHCO_3$ (25 mL) followed by brine (25 mL), dried over Na_2SO_4 and concentrated under reduced pressure. The oily brown crude product was purified by flash column chromatography (SiO_2, dichloro-methane/cyclohexane: 1/1) to afford compound **2** (131 mg, 66 % over two steps) as a brown waxy solid. R_f (dichloromethane/cyclohexane: 1/1) = 0.27, ^{1}H NMR ($CDCl_3$, 400 MHz, 25°C): δ = 7.50–7.33 (m, 10H), 7.04 (d, ^{3}J = 9.2 Hz, 4H), 6.98 (d, ^{3}J = 8.8 Hz, 2H), 6.92 (d, ^{3}J = 8.8 Hz, 4H), 6.86 (d, ^{3}J = 8.8 Hz, 2H), 5.06 (s, 4H); ^{13}C NMR ($CDCl_3$, 100 MHz, 25°C): δ = 155.1, 146.1, 141.3, 137.2, 132.3, 128.7, 128.1, 127.6, 126.1, 122.9, 119.8, 115.8, 70.5; HRMS: *m/z* calcd for $C_{32}H_{26}N_4O_2$: 499.2129 $[M+H]^+$, found 499.2111.

Compound 1,6-4 and 1,7-4: Perylene-3,4:9,10-tetracarboxylic acid bisanhydride (**PDA**, 13.4 g, 34.2 mmol) was dissolved in conc. H_2SO_4 (200 mL) and the solution was heated at 55°C for 19 hours. I_2 (330 mg, 1.30 mmol) was then added to the reaction mixture which was stirred for 6 hours. Br_2 (3.88 mL, 75.3 mmol) was added over 45 min and the mixture was heated at 85°C for 16 hours. After cooling down to room temperature, the reaction mixture was carefully poured into H_2O (1 L). The precipitate was filtered and washed with copious amounts of H_2O, followed by MeOH to afford a crude mixture of 1,6-, 1,7-dibromo and 1,6,7-tribromo isomers as a dark red solid (18.4 g). This crude mixture was used without further purification. ^{1}H NMR analysis in 96–98 % D_2SO_4 in D_2O revealed a ratio of about 24:70:6 of 1,6-, 1,7- and 1,6,7-isomers, respectively.
Acetic acid (20.0 mL, 349 mmol) was added over a suspension of the mixture of 1,6-, 1,7-dibromo and 1,6,7-tribromo isomers (4.00 g, 7.27 mmol) in *N*-methylpyrrolidinone (100 mL) under an argon atmosphere. The mixture was stirred at 60°C for 20 minutes. *N*-Dodecylamine (3.37 g, 18.2 mmol) was then added and the mixture was stirred at 120°C for 12 hours. The resulting dark-red suspension was then poured into water (1 L) to give a precipitate, which was filtered off and washed with MeOH (1 L). The crude product was purified by flash column chromatography (SiO_2, cyclohexane/ethyl acetate: 9/1) to provide a 1:4 regioisomeric mixture of *N,N'*-didodecyl-1,6- and 1,7-dibromoperylene-3,4,9,10-tetracarboxylic acid diimides 1,6:1,7-**4** (3.10 g, 48 % over two steps). R_f (cyclohexane/ethyl acetate: 9/1) = 0.23 (1,6-**4**), 0.18 (1,7-**4**); ^{1}H NMR ($CDCl_3$, 400 MHz, 25°C) of *major 1,7 isomer*: δ = 9.45 (d, ^{3}J = 8.2 Hz, 2H), 8.89 (s, 2H), 8.67 (d, ^{3}J = 8.2 Hz, 2H), 4.20 (t, ^{3}J = 7.6 Hz, 4H), 1.79–1.70 (brm, 4H), 1.46–1.25 (brm, 36H), 0.87 (t, ^{3}J = 6.8 Hz,6H); ^{13}C NMR ($CDCl_3$, 100 MHz, 25 °C) of *major 1,7 isomer*: δ = 163.0, 162.5, 138.1, 133.1, 132.9, 130.1, 129.4, 128.6, 127.1, 123.3, 122.9, 120.9, 41.0, 32.1 (2C), 29.8, 29.8, 29.8, 29.7, 29.5, 28.2, 27.3, 22.8, 14.3; MALDI-TOF: *m/z* calcd for $C_{48}H_{56}Br_2N_2O_4$: 885.267 $[M+H]^+$, found 885.685.

Compound 1,6-5 and 1,7-5: A solution of a 1:4 regioisomeric mixture of 1,6:1,7-**4** (1.30 g, 1.47 mmol) in pyrrolidine (85 mL) was heated at 55°C for 26 hours under an argon atmosphere. The solvent was then evaporated under reduced pressure and the crude product was purified by flash column chromatography (SiO_2, dichloromethane/cyclohexane: 2/1 → 4/1) to give compound 1,6-**5** (170 mg, 13 %) as a dark-blue solid and compound 1,7-**5** (481 mg, 38 %) as a dark-green solid.
*Compound 1,6-**5***: R_f (dichloromethane/cyclohexane: 4:1) = 0.28 (1,6-**5**); ^{1}H NMR ($CDCl_3$, 400 MHz, 25°C): δ = 8.59 (d, ^{3}J = 8.0 Hz, 2H), 8.24 (s, 2H), 7.78 (d, ^{3}J = 8.0 Hz, 2H), 4.21 (t, ^{3}J = 7.6 Hz, 2H), 4.14 (t, ^{3}J = 7.5 Hz, 2H), 3.80–3.46 (brm, 4H), 2.80–2.50 (brm, 4H), 2.20–1.82 (brm, 8H), 1.82–1.54 (brm, 4H), 1.50–1.10 (brm, 36H), 0.88–0.82 (m, 6H); ^{13}C NMR ($CDCl_3$, 100 MHz, 25°C): δ = 164.3, 164.1, 149.9, 135.7, 131.1, 130.2, 128.4, 128.3, 123.3, 122.9, 117.9, 117.6, 117.0, 116.9, 52.2, 40.7, 40.5, 32.0, 30.3, 29.7 (3C), 29.6, 29.5, 29.4, 28.4, 28.3, 27.4, 27.3, 27.0, 25.7, 22.8, 14.2; ESI-MS: *m/z* calcd for $C_{56}H_{72}N_4O_4$: 882.56 $[M+H_2O]^+$, found 882.58;
*Compound 1,7-**5***: R_f (dichloromethane/cyclohexane: 4:1) = 0.22 (1,7-**5**); ^{1}H NMR ($CDCl_3$, 400 MHz, 25°C): δ = 8.39 (s, 2H), 8.33 (d, ^{3}J = 8.0 Hz, 2H), 7.56 (d, ^{3}J = 8.0 Hz, 2H), 4.22 (t, ^{3}J = 7.6 Hz, 4H), 3.82–3.50 (brm, 4H), 2.90–2.65 (brm, 4H), 2.15–1.85 (brm, 8H), 1.83–1.58 (brm, 4H), 1.52–1.10 (brm, 36H), 0.87 (t, ^{3}J = 6.9 Hz, 6H); ^{13}C NMR ($CDCl_3$, 100 MHz, 25°C): δ = 164.2, 146.6, 134.3, 130.0,

126.7, 123.9, 122.2, 121.9, 120.8, 119.2, 118.2, 52.3, 40.7, 32.1, 29.8 (3C), 29.6, 29.5, 28.4, 27.4, 25.9, 22.8, 14.3; HRMS: *m/z* calcd for $C_{56}H_{72}N_4O_4$: 864.5523 $[M+H]^+$, found 864.5554.

Compound 6: A solution of diimide 1,7-**5** (420 mg, 485 □mol) in *tert*-butanol (75 mL) was heated up to reflux under an argon atmosphere. KOH (1.91 g, 34.0 mmol) suspended in hot *tert*-butanol (38 mL) was then added, whereas the dark-green reaction mixture turned blueish green. After heating for 10 minutes, the hot mixture was carefully poured into acetic acid (50 mL) and the mixture turned back dark-green. The reaction mixture was cooled to room temperature and dichloromethane (33 mL) was added. The mixture was washed with H_2O (3 × 80 mL) and the aqueous phases were extracted with dichloromethane (100 mL). The combined organic phases were dried over Na_2SO_4. The solvent was removed under reduced pressure and the resulting crude product was purified by flash column chromatography (SiO_2, chloroform/acetone/*n*-hexane: 10/1/9) to give monoimide **6** (214 mg, 63 %) as a dark-green solid. R_f (chloroform/acetone/*n*-hexane: 10/1/9) = 0.49; ^{1}H NMR ($CDCl_3$, 400 MHz, 25°C): δ = 8.51 (s, 1H), 8.45 (s, 1H), 8.44 (d, ^3J = 8.2 Hz, 1H), 8.41 (d, ^3J = 8.0 Hz, 1H), 7.74 (d, ^3J = 8.0 Hz, 1H), 7.59 (d, ^3J = 8.0 Hz, 1H), 4.22 (t, ^3J = 7.2 Hz, 2H), 3.90–3.60 (brm, 4H), 3.00–2.70 (brm, 4H), 2.20–1.90 (brm, 8H), 1.82–1.68 (m, 2H), 1.50–1.14 (brm, 18H), 0.87 (t, ^3J = 6.8 Hz, 3H); ^{13}C NMR ($CDCl_3$, 100 MHz, 25°C): δ = 164.2, 164.1, 161.5, 161.0, 147.2, 146.5, 136.1, 133.9, 130.6, 130.4, 128.9, 126.7, 124.9, 124.5, 123.9, 122.7, 122.6, 122.3, 121.1, 120.1, 119.8, 117.5, 117.2, 114.6, 52.7, 52.5, 40.8, 32.1, 31.1, 29.9, 29.8, 29.7, 29.6, 29.5, 28.4, 27.3, 26.0 (2C), 22.8, 14.3; HRMS: *m/z* calcd for $C_{44}H_{47}N_3O_5$: 697.3516 $[M]^+$, found 697.3524.

Compound 7: A solution of compound **6** (30 mg, 0.22 mmol) in DMF (1 mL) was added over a solution of 4-aminophenylazide (31 mg, 0.05 mmol) and imidazole (171 mg, 4.15 mmol) in toluene (5 mL), and the resulting mixture was refluxed for 12 h. After cooling to room temperature, chloroform (30 mL) was added. The solution was washed successively with HCl (1%) (20 mL), K_2CO_3sat. (20 mL), water (20 mL) and the organic phase was concentrated under reduced pressure. The crude product was purified by column chromatography (SiO_2, cyclohexane/EtOAc: 1/1) to afford pure compound **7** (31 mg, 85%) as a green solid. R_f (cyclohexane/EtOAc: 1/1) = 0.20; ^{1}H NMR ($CDCl_3$, 400 MHz, 25°C): δ = 8.50 (s, 1H), 8.46 (s, 1H), 8.44 (d, ^3J = 8.1 Hz, 1H), 8.41 (d, ^3J = 8.1 Hz, 1H), 7.69 (d, ^3J = 8.0 Hz, 1H), 7.68 (d, ^3J = 8.0 Hz, 1H),7.13 (d, ^3J = 8.5 Hz, 2H), 6.84 (d, ^3J = 8.5 Hz, 2H), 4.22 (t, ^3J = 7.5 Hz, 2H), 3.82-3.65 (brm, 4H), 2.91-2.75 (brm, 4H), 2.16-1.90 (brm, 8H), 1.81-1.70 (brm, 2H), 1.40-1.19 (brm, 18H), 0.87 (t, ^3J = 6.8 Hz, 3H); ^{13}C NMR ($CDCl_3$, 100 MHz, 25°C): δ = 164.8, 164.7, 164.2, 164.2, 146.8, 146.6, 146.6, 134.5, 134.3, 130.2, 130.1, 129.5, 127.0, 126.8, 126.3, 124.1, 123.8, 122.6, 122.2, 122.1, 121.8, 121.2, 120.8, 119.4, 119.2, 118.4, 118.1, 115.8, 52.3, 40.7, 32.1, 29.8, 29.8, 29.7, 29.6, 29.5, 28.4, 27.3, 27.2, 25.9, 22.8, 14.3.

Compound 8: A solution of *p*-phenylene diamine (293 mg, 2.71 mmol) in dry *N,N'*-dimethylformamide (6 mL) was added over a solution of monoimide **6** (189 mg, 271 □mol) and imidazole (313 mg, 4.60 mmol) in toluene (35 mL) under an argon atmosphere. The mixture was heated up to 150°C for 14 hours. After cooling down to room temperature, chloroform (65 mL) was added. The solution was washed successively with 1 % HCl (40 mL) and sat. Na_2CO_3 (40 mL). The organic phase was dried over Na_2SO_4 and concentrated under reduced pressure. The crude product was purified by flash column chromatography (SiO_2, dichloromethane → dichloromethane/MeOH: 99.5/0.5 → 99/1) to give unsymmetrical diimide **7** (208 mg, quantitative) as a dark-green solid. R_f (dichloromethane/methanol: 99/1) = 0.19; ^{1}H NMR ($CDCl_3$, 400 MHz, 25°C): δ = 8.47 (s, 1H), 8.41 (s, 1H), 6.39 (d, ^3J = 8.5 Hz, 1H), 6.37 (d, ^3J = 8.2 Hz, 1H), 7.62 (d, ^3J = 8.3 Hz, 1H), 7.60 (d, ^3J = 8.8 Hz, 1H), 7.15 (d, ^3J = 8.4 Hz, 2H), 6.87 (d, ^3J = 8.4 Hz, 2H), 4.22 (t, ^3J = 7.2 Hz, 2H), 3.90–3.50 (brm, 4H), 2.95–2.60 (brm, 4H), 2.20–1.85 (brm, 8H), 1.80–1.69 (m, 2H), 1.52–1.19 (m, 18H), 0.87 (t, ^3J = 6.8 Hz, 3H); ^{13}C NMR ($CDCl_3$, 100 MHz, 25°C): δ = 164.8, 164.7, 164.3, 164.2, 146.7, 146.6, 146.4, 134.6, 134.3, 130.2, 130.1, 129.5, 127.1, 126.8, 126.6, 124.1, 123.9, 122.7, 122.2, 122.1, 121.9, 121.2, 120.9, 119.4, 119.3, 118.5, 118.1, 116.1, 52.3 (2C), 32.1, 29.8, 29.8 (2C), 29.7, 29.6, 29.5, 28.4, 27.4, 26.0, 22.8, 14.3; HRMS: *m/z* calcd for $C_{50}H_{53}N_5O_4$: 788.4181 $[M+H]^+$, found 788.4170.

Compound 9: A solution of diimide **7** (208 mg, 264 μmol) and triethylamine (36.8 μL, 264 μmol) in dry dichloromethane (7 mL) was added slowly over a solution of 2-chloroacetyl chloride (21.0 μL, 264 μmol) in dry dichloromethane (1.6 mL) at 0°C under an argon atmosphere. The reaction mixture was stirred for 2 hours at room temperature and then further dissolved in Et_2O (40 mL). The organic phase was extracted with sat. NH_4Cl (20 mL), brine (20 mL) and dried over Na_2SO_4. After concentration under reduced pressure, the crude product was purified by a short column (SiO_2, ethyl acetate/*n*-hexane: 1/1) to afford compound **8** (203 mg, 89 %) as a dark-green solid, which was pure enough to be used as such in the next step. R_f (dichloro-methane/methanol: 99/1) = 0.18; ^{1}H NMR ($CDCl_3$, 400 MHz, 25°C): δ = 8.51 (s, 1H), 8.44 (s, 1H), 8.37–8.31 (m, 3H), 7.76 (d, ^3J = 8.7 Hz, 2H,), 7.55 (d, ^3J = 8.0 Hz, 1H), 7.49 (d, ^3J = 8.0 Hz, 1H), 7.41 (d, ^3J = 8.7 Hz, 2H), 4.23–4.18 (m, 4H), 3.80–3.56 (brm, 4H), 2.89–2.60 (brm, 4H), 2.14–1.86 (brm, 8H), 1.81–1.69 (m, 2H), 1.50–1.15 (brm, 18H), 0.87 (t, ^3J = 6.8 Hz, 3H); ^{13}C NMR ($CDCl_3$, 100 MHz, 25°C): δ = 171.1, 164.6, 164.5, 164.3, 164.3, 146.8, 146.6, 137.1, 134.9, 134.2, 132.5, 130.2, 130.1, 129.7, 127.3, 126.8, 124.2, 123.9, 122.7, 122.2, 122.0, 121.7, 121.3, 121.0, 119.3, 118.9, 118.7, 117.9, 52.4, 52.4, 43.1, 40.7, 32.1, 29.8, 29.8, 29.7, 29.6, 29.5, 28.4, 27.3, 25.9, 22.8, 14.2; HRMS: *m/z* calcd for $C_{52}H_{54}ClN_5O_5$: 863.3813 $[M]^+$, found 863.3795.

Compound 10: A solution of compound **9** (203 mg, 235 μmol) and NaN_3 (214 mg, 3.29 mmol) in dry *N,N'*-dimethylformamide (8 mL) was heated at 80°C for 25 hours. After cooling down to room temperature, chloroform (65 mL) was added and the mixture was extracted with H_2O (3 × 45 mL). The combined aqueous phases were extracted with chloroform (3 × 45 mL). The combined organic phases were dried over Na_2SO_4 and concentrated under reduced pressure. The resulting crude product was purified by flash column chromatography (SiO_2, cyclohexane/ethyl acetate: 1/1) to give azide **10** (143 mg, 70 %) as a dark-green solid. R_f (cyclohexane/ethyl acetate: 1/1) = 0.37; ^{1}H NMR ($CDCl_3$, 400 MHz, 25°C): δ = 8.45 (s, 1H), 8.40 (s, 1H), 8.33 (d, ^3J = 8.1 Hz, 1H), 8.29 (d, ^3J = 8.4 Hz, 1H), 8.28 (s, 1H), 7.71

(d, ^3J = 8.7 Hz, 2H), 7.50 (d, ^3J = 8.0 Hz, 1H), 7.42 (d, ^3J = 8.1 Hz, 1H), 7.38 (d, ^3J = 8.7 Hz, 2H), 4.21 (t, ^3J = 7.5 Hz, 2H), 4.11 (s, 2H) 3.72-3.55 (brm, 4H), 2.82-2.60 (brm, 4H), 2.10-1.85 (brm, 8H), 1.81-1.69 (brm, 2H), 1.32-1.18 (brm, 18H), 0.87 (t, ^3J = 6.8 Hz, 3H); ^{13}C NMR ($CDCl_3$, 100 MHz, 25°C): δ = 165.0, 164.4, 164.4, 164.0, 164.0, 146.6, 146.3, 137.5, 134.5, 133.7, 132.0, 129.9, 129.7, 129.4, 127.0, 126.6, 124.1, 123.6, 122.5, 121.9, 121.8, 121.6, 121.0, 120.9, 120.7, 119.2, 118.8, 118.5, 117.5, 53.0, 52.3, 52.2, 43.6, 40.7, 32.0, 30.3, 29.8, 29.8, 29.7, 29.6, 29.5, 28.3, 27.3, 27.0, 25.9, 22.8, 14.2; HRMS: *m/z* calcd for $C_{52}H_{54}N_8O_5$: 870.4217 $[M]^+$, found 870.4193.

Compound 14: To a solution of pseudorotaxane **11** (78.9 mg, 53.8 µmol), azide **3** (29.9 mg, 53.8 µmol), azide **10** (46.9 mg, 53.8 µmol), $Cu(MeCN)_4PF_6$ (40.1 mg, 108 µmol) in dry dichloromethane (1.6 mL), 2,6-lutidine (1.24 µL, 10.8 µmol) was added under an argon atmosphere. The dark-green solution was stirred at room temperature for 3 days. The reaction mixture was then evaporated and the crude product was purified by flash column chromatography (SiO_2, dichloromethane/methanol /toluene: 100/0/2 → 100/5/2) to give compound **14** (38.8 mg, 25 %) as a dark-green solid. R_f (dichloromethane/methanol/toluene: 100/6/2) = 0.27; ^{1}H NMR ($CDCl_3$, 400 MHz, 25°C): δ = 8.90 (brs, 1H), 8.42 (brs, 1H), 8.40–8.16 (m, 4H), 7.82–7.62 (m, 2H), 7.61–7.49 (m, 3H), 7.49–7.42 (m, 1H), 7.42–7.27 (m, 14H), 6.93 (d, ^3J = 8.8 Hz, 4H), 6.89–6.59 (m, 18H,), 6.59–6.49 (m, 2H), 5.25 (brs, 2H), 5.18 (brs, 2H), 4.96 (brs, 4H), 4.68–4.25 (m, 6H), 4.25–3.47 (m, 52H), 3.47–3.24 (m, 4H), 2.89–2.43 (m, 8H), 2.14–1.81 (m, 8H), 1.81–1.52 (m, 12H), 1.51–1.01 (brm, 24H), 0.97–0.67 (brm, 3H); ^{13}C NMR ($CDCl_3$, 100 MHz, 25°C): δ = 167.8, 164.5, 164.4, 164.2, 164.0, 163.7, 154.9, 148.2, 147.7, 147.6, 146.7, 146.5, 146.4 (2C), 146.2, 145.6, 141.4, 137.9, 137.2, 134.7, 133.9, 132.5 (2C), 132.0, 131.0, 130.9, 129.4, 129.0, 128.7, 128.1, 127.6, 126.5, 126.0, 124.1, 123.8, 123.0 (2C), 122.5, 122.0, 121.4, 121.2, 121.1, 120.8, 119.4, 118.6, 117.6, 115.7, 113.0, 113.0, 112.7, 111.9, 72.3, 72.0, 70.8, 70.4, 67.6, 67.1, 66.9 (2C), 53.1 (2C), 52.3 (2C), 52.2, 48.9, 40.8, 38.9, 37.2, 32.0, 29.8, 29.6, 29.5, 29.1, 28.9, 28.4, 26.6, 26.4, 25.9, 25.4, 23.1, 22.8, 14.2; ESI-MS: *m/z* calcd for $C_{152}H_{179}F_{12}N_{15}O_{24}P_2$: 1299.664 $[M–2PF_6]^{2+}$, found 1299.645.

Compound 15: To a solution of pseudorotaxane **11** (50.3 mg, 34.4 µmol), azide **2** (17.2 mg, 34.4 µmol), azide **10** (30.0 mg, 34.4 µmol), $Cu(MeCN)_4PF_6$ (25.6 mg, 34.4 µmol) in dry dichloromethane (1.2 mL), one drop of 2,6-lutidine was added under an argon atmosphere. The dark-green solution was stirred at room temperature for 3 days. The reaction mixture was then evaporated and the crude was purified by flash column chromatography (SiO_2, dichloromethane/methanol/toluene: 100/0/2 → 100/6/2) to give compound **15** (10.1 mg, 10 %) as a dark-green solid. R_f (dichloromethane/methanol/toluene: 100/6/2) = 0.14; ^{1}H NMR (CD_3CN, 400 MHz, 25°C): δ = 9.09 (s, 1H), 8.18 (s, 1H), 8.10 (d, ^3J = 8.0 Hz, 1H), 8.03 (s, 1H), 8.02 (d, ^3J = 8.4 Hz,1H), 7.82 (s, 2H), 7.78 (d, ^3J = 8.8 Hz, 2H), 7.64 (s, 2H), 7.50 – 7.28 (m, 14H), 7.28–7.20 (m, 2H), 6.99 (d, ^3J = 9.2 Hz, 4H), 6.91 (d, ^3J = 9.2 Hz, 4H), 6.81 (d, ^3J = 8.8 Hz, 2H), 6.84–6.58 (m, 12H), 6.44–6.36 (m, 2H), 5.26 (s, 2H), 5.02 (brs, 4H), 4.60–4.32 (m, 4H), 4.31–3.55 (m, 50H), 3.55–3.28 (m, 8H), 2.68 (t, ^3J = 7.4 Hz, 2H), 2.63 (t, ^3J = 7.3 Hz, 2H), 2.60–2.40 (m, 4H), 2.32–1.48 (m, 20H), 1.48–0.99 (brm, 24H), 0.99–0.71 (brm, 3H); ^{13}C NMR ($CDCl_3$, 100 MHz, 25°C): δ = 165.7, 165.1, 165.0, 164.5, 156.8, 150.0, 149.2, 148.7 (3C), 147.3, 147.2, 147.1 (2C), 146.9, 141.2, 139.1, 138.3, 134.9, 134.2, 133.6, 130.8, 130.7, 130.6, 130.3, 129.5, 129.0, 128.6, 128.2, 127.4, 127.1, 126.4, 126.3, 124.8, 124.4, 124.1, 123.6 (2C), 123.0, 122.5, 122.3 (2C), 122.1, 121.7, 121.3, 121.0, 120.4, 119.7 (2C), 116.9, 114.3, 113.1, 113.0, 112.8 (2C), 73.1, 73.0, 71.6 (2C), 71.5, 71.4, 71.3, 71.1, 71.0, 68.6, 68.4, 68.3, 68.1 (2C), 68.0, 53.5, 53.0, 52.9, 52.7, 52.6, 49.8, 49.7, 41.1, 34.3, 32.7, 30.4, 30.3, 30.2, 30.1, 30.0, 29.8, 29.7, 28.9, 28.8, 27.9, 27.2, 26.9, 26.4, 26.0, 25.9, 23.4, 14.4; HRMS: *m/z* calcd for $C_{150}H_{176}F_{12}N_{14}O_{23}P_2$: 1271.1528 $[M–2PF_6]^{2+}$, found 1271.1500.

Compound 16^{Ext}: *First step:* To a solution of rotaxane **14** (29.7 mg, 10.3 µmol) in dry dichloromethane (1.56 mL), methyl iodide (0.51 mL) was added at once under an argon atmosphere. The dark-green solution was stirred at room temperature for 4 days and the solvent was then evaporated to give the diiodide precursor of **16^{Ext}** as a dark-green solid (33 mg). ^{1}H NMR (CD_3CN, 400 MHz, 25°C): δ = 9.81 (s, 1H), 9.34 (s, 1H), 8.46 (s, 1H), 8.37 (s, 1H), 8.20 (s, 1H), 8.13 (d, ^3J = 8.0 Hz, 1H), 8.06 (s, 1H), 8.05 (d, ^3J = 8.0 Hz, 1H), 7.89 (d, ^3J = 8.4 Hz, 2H), 7.46 (d, ^3J = 8.4 Hz, 2H), 7.44–7.24 (m, 14H), 6.98–6.83 (m, 8H), 6.83–6.60 (m, 14H), 6.48–6.38 (m, 2H), 5.71 (s, 2H), 5.55 (s, 2H), 5.00 (s, 4H), 4.60–4.36 (m, 4H), 4.34–3.57 (m, 50H), 4.19 (s, 3H), 4.14 (s, 3H), 3.57–3.34 (brm, 8H,), 2.77 (t, ^3J = 7.2 Hz, 2H), 2.70 (t, ^3J = 7.4 Hz, 2H), 2.70–2.40 (brm, 4H), 2.08–1.80 (brm, 8H), 1.80–1.50 (m, 12H), 1.50–1.15 (brm, 24H), 0.92–0.80 (m, 3H); ^{13}C NMR (CD_3CN, 400 MHz, 25°C): δ = 165.1, 165.0, 164.5, 164.5, 162.8, 162.0, 156.0, 148.0 (2C), 147.3, 147.2, 147.1 (3C), 146.9, 146.7, 145.7, 145.6, 142.1, 138.7, 138.4, 135.0, 134.2, 134.0, 132.2, 132.0, 130.9, 130.9, 130.5 (2C), 130.4, 129.7, 129.5, 128.9, 128.6, 128.4, 127.1, 126.3 (2C), 124.8, 124.4, 123.7, 123.6, 123.1, 122.5, 122.3 (2C), 122.0, 121.7, 121.3 (2C), 121.0, 119.8, 119.7, 119.0, 118.0, 116.7, 114.3, 113.2, 113.1, 112.9, 73.1 (2C), 71.6 (2C), 71.5 (3C), 71.3, 71.2, 70.9, 68.6, 68.4, 68.3, 68.2 (2C), 68.1, 68.0, 67.0, 66.6, 56.6, 56.4, 52.9, 52.7, 52.6, 49.7, 41.1, 38.8, 38.7, 32.7, 30.4 (2C), 30.3 (2C), 30.2, 30.1, 30.0, 28.8 (2C), 27.9, 27.5, 27.4, 27.3, 27.2, 26.9 (2C), 23.8, 23.7, 23.4, 14.4.

Second step: To a suspension of the previous solid in water (1.4 mL) were added NH_4PF_6 (13.4 mg, 82.4 µmol) and dry dichloromethane (1.4 mL). The resulting biphasic solution was vigorously stirred for 1 hour. The aqueous phase was extracted with dichloromethane (3 × 1.6 mL). The combined organic phases were dried over Na_2SO_4 and evaporated under reduced pressure to give rotaxane **16^{Ext}** (26.5 mg, 80 %) as a dark-green solid. ^{1}H NMR (CD_3CN, 400 MHz, 25°C): δ = 9.26 (s, 1H, $H_{am'}$), 8.83 (s, 1H, H_{am}), 8.28 (s, 1H, $H_{T1\ or\ T1'}$), 8.24 (s, 1H, $H_{A'\ or\ D'}$), 8.19 (s, 1H, $H_{T1\ or\ T1'}$), 8.16 (d, ^3J = 8.0 Hz, 1H, $H_{B',\ ortho\ or\ C',\ ortho}$), 8.08 (s, 1H, $H_{A'\ or\ D'}$), 8.06 (d, ^3J = 8.0 Hz, 1H, $H_{B',\ ortho\ or\ C',\ ortho}$), 7.80 (d, ^3J = 8.8 Hz, 2H, $H_{E1'\ or\ E2'}$), 7.48 (d, ^3J = 8.8 Hz, 2H, $H_{E1'\ or\ E2'}$), 7.46–7.26 (m, 14H, H_C $H_{A1\ or\ A2}$ $H_{B',\ bay\ or\ C',\ bay}$), 6.98–6.86 (m, 8H, H_{B1} H_{B2}), 6.83–6.60 (m, 14H, $H_{A1\ or\ A2}$ $H_{ar,\ DB24C8}$), 6.49–6.39 (m, 2H, $H_{ar,\ DB24C8}$), 5.53 (s, 2H, H□'), 5.39 (s, 2H, H□), 5.03 (s, 4H, H□), 4.58–4.36 (m, 4H, H_9 $H_{9'}$), 4.34–3.61 (m, 50H, $H_{CH2O,\ DB24C8}$ $H_{im1'}$), 4.19 (s, 3H, $H_{Me\ or\ Me'}$), 4.14 (s, 3H, $H_{Me\ or\ Me'}$), 3.62–3.34 (brm, 8H, $H_{F'\ or\ G'}$ H_8 $H_{8'}$), 2.76 (t, ^3J = 7.8 Hz, 2H, $H_{3\ or\ 3'}$), 2.69 (t, ^3J = 7.8 Hz, 2H, $H_{3\ or\ 3'}$), 2.75–2.45 (brm, 4H, $H_{F'\ or\ G'}$), 2.08–1.80 (brm, 8H, $H_{F'\ or\ G'}$), 1.80–1.50 (m, 12H, $H_{im2'}$ H_4 $H_{4'}$ H_7 $H_{7'}$), 1.50–1.15 (brm, 24H, H_5 $H_{5'}$ H_6 $H_{6'}$ $H_{im2'}$), 0.92–0.80 (m, 3H, $H_{Me'}$); ^{13}C NMR (CD_3CN, 400 MHz, 25°C): δ = 165.1 (2C), 164.5, 164.5, 162.8, 162.0, 156.1, 148 (2C), 147.3, 147.2 (2C), 147.1 (2C), 147.0, 146.8,

145.8, 145.7, 142.1, 138.6, 138.5, 135.1, 134.3, 134.2, 132.3, 131.8, 131.0, 130.7, 130.4, 129.5, 128.9, 128.7, 127.4, 127.2, 127.1, 126.3 (2C), 124.9, 124.4, 123.7, 123.6, 123.1, 122.6, 122.3, 122.2, 122.0, 121.7, 121.3 (2C), 121.0, 119.8 (2C), 119.0, 118.1, 116.8, 114.3, 113.1 (2C), 112.8, 73.1, 73.0, 71.6 (2C), 71.5 (3C), 71.3, 71.1, 70.9, 68.6, 68.3 (2C), 68.2 (2C), 68.1, 68.0, 56.3, 56.2, 52.9, 52.7, 52.6, 49.7 (2C), 41.1, 38.7, 38.6, 32.7, 30.4 (2C), 30.3 (2C), 30.1, 28.9, 28.8, 27.9, 27.4 (2C), 27.3, 27.2, 26.9 (2C), 26.4 (2C), 23.8, 23.7, 23.4, 14.4; ESI-MS: *m/z* calcd for $C_{154}H_{185}F_{24}N_{15}O_{24}P_4$: 657.343 $[M–4PF_6]^{4+}$, found 657.317.

Compound 17^{Ext}: To a solution of rotaxane **15** (13.5 mg, 4.77 µmol) in dry dichloromethane (0.7 mL), methyl iodide (237 µL) was added at once under an argon atmosphere. After 4 days, MeI (60 µL) was added and the mixture was stirred for 1 day, then the solvent was evaporated. To a suspension of the previous solid in water (0.6 mL) were added NH_4PF_6 (6.2 mg, 38.1 µmol) and dry dichloromethane (0.6 mL). The resulting biphasic solution was vigorously stirred for 1 hour. The aqueous phase was extracted with dichloromethane (3 × 0.7 mL). The combined organic phases were dried over Na_2SO_4 and evaporated under reduced pressure to give compound **17^{Ext}** (14.2 mg, 94 %) as a dark-green solid. ^{1}H NMR (CD_3CN, 400 MHz, 25°C): δ = 9.28 (s, 1H, $H_{am'}$), 8.40 (s, 1H, $H_{T1\ or\ T1'}$), 8.28 (s, 1H, $H_{T1\ or\ T1'}$), 8.25 (s, 1H, $H_{A'\ or\ D'}$), 8.17 (d, ^3J = 8.0 Hz, 1H, $H_{B',\ ortho\ or\ C',\ ortho}$), 8.07 (s, 1H, $H_{A'\ or\ D'}$), 8.06 (d, ^3J = 8.0 Hz, 1H, $H_{B',\ ortho\ or\ C',\ ortho}$), 7.80 (d, ^3J = 8.8 Hz, 2H, $H_{E1'\ or\ E2'}$), 7.54 (d, ^3J = 8.8 Hz, 2H, $H_{A1\ or\ A2}$), 7.49 (d, ^3J = 8.4 Hz, 2H, $H_{E1'\ or\ E2'}$), 7.51–7.27 (m, 14H, H_C $H_{B',\ bay\ or\ C',\ bay}$), 7.15 (d, ^3J = 9.2 Hz, 4H, $H_{B1\ or\ B2}$), 7.01 (d, ^3J = 9.2 Hz, 4H, $H_{B1\ or\ B2}$), 6.98–6.59 (m, 12H, $H_{ar,\ DB24C8}$), 6.88 (d, ^3J = 9.6 Hz, 2H, $H_{A1\ or\ A2}$), 6.49–6.38 (m, 2H, $H_{ar,\ DB24C8}$), 5.54 (s, 2H, H□'), 5.08 (s, 4H, H□), 4.60–4.35 (m, 4H, H_9 $H_{9'}$), 4.34–3.61 (m, 50H, $H_{CH2O,\ DB24C8}$ $H_{im1'}$), 4.19 (s, 3H, $H_{Me\ or\ Me'}$), 4.16 (s, 3H, $H_{Me\ or\ Me'}$), 3.62–3.32 (brm, 8H, $H_{F'\ or\ G'}$ H_8 $H_{8'}$), 2.76 (t, ^3J = 7.6 Hz, 2H, $H_{3\ or\ 3'}$), 2.71 (t, ^3J = 7.6 Hz, 2H, $H_{3\ or\ 3'}$), 2.82–2.47 (brm, 4H, $H_{F'\ or\ G'}$), 2.08–1.80 (brm, 8H, $H_{F'\ or\ G'}$), 1.80–1.50 (m, 12H, $H_{im2'}$ H_4 $H_{4'}$ H_7 $H_{7'}$), 1.50–1.15 (brm, 24H, H_5 $H_{5'}$ H_6 $H_{6'}$ $H_{im2'}$), 0.92–0.80 (m, 3H, $H_{Me'}$); ^{13}C NMR (CD_3CN, 100 MHz, 25°C): δ = 165.1, 165.0, 164.5, 162.7, 157.6, 152.8, 148.8, 148.7, 147.2 (2C), 147.1, 147 (3C), 146.1, 145.8, 140.1, 138.6, 138.2, 135.0, 134.2, 134.1, 131.0, 130.8, 130.7, 130.4, 129.6, 129.2, 129.0, 128.7, 128.2, 127.4, 127.1, 126.8, 126.3, 126.2, 124.8, 124.4, 123.7, 123.6, 123.2, 121.7, 121.3, 121.2, 120.9, 119.8, 118.9, 117.1, 114.2, 113.1, 112.8, 73.0, 71.6, 71.5 (2C), 71.3, 71.1, 70.9 (2C), 68.6, 68.3, 68.1, 68.0 (2C), 56.3, 52.9, 52.7, 52.6, 49.7, 41.1, 38.7, 38.4, 34.2, 32.7, 30.4, 30.3, 30.2, 30.1, 29.8, 28.9, 28.8, 27.9, 27.8, 27.4, 27.3, 27.0, 26.9, 26.4, 25.6, 23.7, 23.4, 14.4; HRMS: *m/z* calcd for $C_{152}H_{182}F_{24}N_{14}O_{23}P_4$: 1431.1404 $[M–2PF_6]^{2+}$, found 1431.1465.

General protocol for the contraction of rotaxane 16^{Ext} and 17^{Ext}: To a solution of the extended rotaxane in dry dichloromethane (2 mL, 1 mM), an aqueous solution of 0.1 M NaOH (2 mL) was added dropwise and the mixture was vigorously stirred at room temperature for 1 hour. The organic phase was then separated, dried over Na_2SO_4 and concentrated under reduced pressure. The residual solid was triturated with MeOH, filtered and washed with pentane to give the contracted rotaxane as a dark-green solid.

General protocol for the extension of rotaxane 16^{Cont} and 17^{Cont}: To a solution of the contracted rotaxane in chloroform (2 mL, 1 mM) was added 2 equivalents of TFA. The solution was briefly stirred before evaporating the solvents. The residue was taken back in a 1:1 mixture of chloroform/aqueous $NH_4PF_{6\ sat.}$ (2 mL) and stirred vigorously for one hour. The mixture was extracted with chloroform, the organic phase dried with sodium sulfate, filtered, and evaporated to yield the extended rotaxane as a dark-green solid.

Acknowledgements

This work was performed within the framework of the IRTG “Soft Matter Science: Concepts for the Design of Functional Materials” (A.W., S. L. and N.G.). We wish to thank the international center for Frontier Research in Chemistry (fellowship to A.W.) and the Laboratory of Excellence for Complex System Chemistry. This work was also supported by the Agence Nationale pour la Recherche (ANR-09-BLAN-034-02), the French Ministry of Research and the China Scholarship Council (fellowships to J.J.C., F.N. and G. D. respectively).

Keywords: rotaxane • triarylamine • perylene • pH-responsive • electroactive

[1] C. J. Bruns, J. F. Stoddart, *The Nature of the Mechanical Bond*, John Wiley & Sons, Inc., Hoboken, NJ, USA, **2016**.
[2] S. Erbas-Cakmak, D. A. Leigh, C. T. McTernan, A. L. Nussbaumer, *Chem. Rev.* **2015**, *115*, 10081–10206.
[3] A. Coskun, M. Banaszak, R. D. Astumian, J. F. Stoddart, B. A. Grzybowski, *Chem. Soc. Rev.* **2012**, *41*, 19–30.
[4] M. C. Jiménez, C. Dietrich-Buchecker, J.-P. Sauvage, *Angew. Chem. Int. Ed.* **2000**, *39*, 3284–3287.
[5] L. Fang, M. Hmadeh, J. Wu, M. A. Olson, J. M. Spruell, A. Trabolsi, Y. W. Yang, M. Elhabiri, A. M. Albrecht-Gary, J. F. Stoddart, *J. Am. Chem. Soc.* **2009**, *131*, 7126–7134.
[6] P. G. Clark, M. W. Day, R. H. Grubbs, *J. Am. Chem. Soc.* **2009**, *131*, 13631–13633.
[7] L. Gao, Z. Zhang, B. Zheng, F. Huang, *Polym. Chem.* **2014**, *5*, 5734–5739.
[8] G. Du, E. Moulin, N. Jouault, E. Buhler, N. Giuseppone, *Angew. Chem. Int. Ed.* **2012**, *51*, 12504–12508.
[9] A. Goujon, G. Du, E. Moulin, G. Fuks, M. Maaloum, E. Buhler, N. Giuseppone, *Angew. Chem. Int. Ed.* **2016**, *55*, 703–707.
[10] A. Goujon, G. Mariani, T. Lang, E. Moulin, M. Rawiso, E. Buhler, N. Giuseppone, *J. Am. Chem. Soc.* **2017**, *139*, 4923–4928.
[11] A. Goujon, T. Lang, G. Mariani, E. Moulin, G. Fuks, J. Raya, E. Buhler, N. Giuseppone, *J. Am. Chem. Soc.* **2017**, *139*, 14825–14828.
[12] K. Iwaso, Y. Takashima, A. Harada, *Nat. Chem.* **2016**, *8*, 625–632.
[13] S. Ikejiri, Y. Takashima, M. Osaki, H. Yamaguchi, A. Harada, *J. Am. Chem. Soc.* **2018**, *140*, 17308–17315.

[14] A. Goujon, E. Moulin, G. Fuks, N. Giuseppone, *CCS Chem.* **2019**, accepted for publication.
[15] A. Wolf, E. Moulin, J. J. Cid Martín, A. Goujon, G. Du, E. Busseron, G. Fuks, N. Giuseppone, *Chem. Commun.* **2015**, *51*, 4212–4215.
[16] Q. Zhang, S.-J. Rao, T. Xie, X. Li, T.-Y. Xu, D.-W. Li, D.-H. Qu, Y.-T. Long, H. Tian, *Chem* **2018**, DOI:10.1016/j.chempr.2018.08.030.
[17] Z. Ning, H. Tian, *Chem. Commun.* **2009**, 5483.
[18] V. Faramarzi, F. Niess, E. Moulin, M. Maaloum, J.-F. Dayen, J.-B. Beaufrand, S. Zanettini, B. Doudin, N. Giuseppone, *Nat. Chem.* **2012**, *4*, 485–490.
[19] J. J. Armao, M. Maaloum, T. Ellis, G. Fuks, M. Rawiso, E. Moulin, N. Giuseppone, *J. Am. Chem. Soc.* **2014**, *136*, 11382–11388.
[20] J. J. Armao, Y. Domoto, T. Umehara, M. Maaloum, C. Contal, G. Fuks, E. Moulin, G. Decher, N. Javahiraly, N. Giuseppone, *ACS Nano* **2016**, *10*, 2082–2090.
[21] J. J. Armao, P. Rabu, E. Moulin, N. Giuseppone, *Nano Lett.* **2016**, *16*, 2800–2805.
[22] T. K. Ellis, M. Galerne, J. J. Armao, A. Osypenko, D. Martel, M. Maaloum, G. Fuks, O. Gavat, E. Moulin, N. Giuseppone, *Angew. Chem. Int. Ed.* **2018**, *57*, 15749–15753.
[23] E. Moulin, J. J. Armao, N. Giuseppone, *Acc. Chem. Res.* **2019**, *52*, DOI:10.1021/acs.accounts.8b00536.
[24] R. K. Dubey, A. Efimov, H. Lemmetyinen, *Chem. Mater.* **2011**, *23*, 778–788.
[25] R. K. Dubey, M. Niemi, K. Kaunisto, A. Efimov, N. V. Tkachenko, H. Lemmetyinen, *Chem. Eur. J.* **2013**, *19*, 6791–6806.
[26] J. Feng, D. Wang, H. Wang, D. Zhang, L. Zhang, X. Li, *J. Phys. Org. Chem.* **2011**, *24*, 621–629.
[27] M. J. Fuller, L. E. Sinks, B. Rybtchinski, J. M. Giaimo, X. Li, M. R. Wasielewski, *J. Phys. Chem. A* **2005**, *109*, 970–975.
[28] Y. Shibano, T. Umeyama, Y. Matano, N. V. Tkachenko, H. Lemmetyinen, Y. Araki, O. Ito, H. Imahori, *J. Phys. Chem. C* **2007**, *111*, 6133–6142.
[29] M. Berberich, A.-M. Krause, M. Orlandi, F. Scandola, F. Würthner, *Angew. Chem. Int. Ed.* **2008**, *47*, 6616–6619.
[30] F. Coutrot, *ChemistryOpen* **2015**, 10.1002/open.201500088.
[31] F. Coutrot, C. Romuald, E. Busseron, *Org. Lett.* **2008**, *10*, 3741–3744.
[32] E. Busseron, J.-J. Cid, A. Wolf, G. Du, E. Moulin, G. Fuks, M. Maaloum, P. Polavarapu, A. Ruff, A.-K. Saur, et al., *ACS Nano* **2015**, *9*, 2760–2772.
[33] F. Würthner, V. Stepanenko, Z. Chen, C. R. Saha-Möller, N. Kocher, D. Stalke, *J. Org. Chem.* **2004**, *69*, 7933–7939.
[34] W. Zhu, D. Ma, *Chem. Commun.* **2004**, 888–889.
[35] From 1D and 2D NMR it was not possible to determine proton B3 and B4. However, considering the electron density of nitrogen and oxygen atoms, we believe that the higher field doublet corresponds to H_{B4} while the lower field one would be H_{B3}.
[36] P. Blanchard, C. Malacrida, C. Cabanetos, J. Roncali, S. Ludwigs, *Polym. Int.* **2019**, DOI:10.1002/pi.5695.
[37] O. Yurchenko, D. Freytag, L. zur Borg, R. Zentel, J. Heinze, S. Ludwigs, *J. Phys. Chem. B* **2012**, *116*, 30–39.
[38] G. Ragazzon, C. Schäfer, P. Franchi, S. Silvi, B. Colasson, M. Lucarini, A. Credi, *Proc. Natl. Acad. Sci.* **2018**, *115*, 9385–9390